Journal of the Meteorological Society of Japan, Vol. 76, No. 4, pp. 517–531, 1998

Trends and Inter-Decadal Variations of the Surface and Lower-Tropospheric Temperature in the Northern Hemisphere from 1964 to 93

By Tetsuzo Yasunari,[1] Motoki Nishimori

Institute of Geoscience, University of Tsukuba, Ibaraki 305-8571, Japan

and

Tetsuji Mito[2]

Master Program of the Environmental Sciences, University of Tsukuba

(Manuscript received 30 August 1996, in revised form 27 April 1998)

Abstract

In this study, we demonstrate remarkable warming trends in northern winter and spring not only at the surface but also in the lower troposphere during a recent 30 year period (1964–93). In winter, major warming has happened over central Siberia and the northwestern Canada/Alaska region. The vertical structure of the warming tendency is somewhat different between these two regions. In spring, tropospheric warming is most noticeable over the northern part of North America. A three-dimensional rotated EOF analysis of the temperature anomaly field in these seasons confirmed the warming trends as the most dominant mode at the surface and in the lower troposphere.

The rotated EOF analysis also shows that an interdecadal-scale fluctuation with abrupt changes in the periods of 1976/77 and 1988/89 is another dominant mode in the temperature field in winter. The spatial structure of this mode shows a wavenumber-three spatial pattern with positive factorloadings over North America, Northern Europe and the eastern part of Eurasia. In spring, a fluctuation of 10–13 year period is noticed in the second largest mode, which suggests a possible relation with the solar cyle of the same period. Possible forcing factors of these tropospheric temperature trends and fluctuations are briefly discussed.

1. Introduction

The greenhouse gases, *i.e.*, CO_2, CH_4 *etc.*, have steadily been increasing because of human activity. The potential for global warming due to the enhanced greenhouse effect has been particularly noted in recent years. The atmospheric GCM experiments with doubled CO_2 concentration have suggested a considerable increase of tropospheric temperature, particularly in the high latitudes (*e.g.*, IPCC, 1996). The transient response experiments by some coupled atmosphere-ocean GCMs with increasing CO_2 at the current rate have predicted a global surface temperature increase of 1 to 2°C by 2050. In the real climate system, the global and hemispheric surface air temperature have shown an apparent increasing trend in the past 100 years, though the overall features in time change and spatial pattern of this increasing trend are somewhat different from those predicted by the GCM experiments (IPCC, 1996 *etc.*).

The long-term variations of hemispheric or regional surface air temperature are shown by many studies (*e.g.*, Jones and Briffa, 1992; Hansen and Lebedeff, 1987; Jones, 1994a; Parker *et al.*, 1994). However, to detect the temperature increase due to the increasing greenhouse effect, the tropospheric temperature, particularly in the lower part, should be examined, rather than only the surface air temperature. The surface air temperature, in addition, is more or less affected by local effects, *e.g.*, urbanization, location changes of stations, *etc.*

Few researchers so far have attempted to detect the global or hemispheric temperature change in the troposphere, owing to the smaller number of available stations and shorter-period data coverage when

1 Corresponding author: Prof. T. Yasunari, Institute of Geoscience, University of Tsukuba, Ibaraki 305-8571, Japan. E-mail: yasunari@atm.geo.tsukuba.ac.jp

2 Present affiliation: Tokyo Electric Power Cooperation

compared to the surface temperature data. Angell (1988) examined the zonal mean tropospheric temperature for the period 1958 to 1987, and found a general increase of temperature in the mid-latitudes (30°–60°N) during the more recent 15 years (1973–1987). Oort and Liu (1993) updated the zonally averaged tropospheric temperature, and confirmed the increasing trend of mid-tropospheric temperature (850–300 hPa) particularly in mid latitudes. On the other hand, Jones (1994b) calculated linear trends of global-mean temperature for 1979 to 1993, and noted a significant warming trend at the surface level but no remarkable tendencies in the troposphere. Some recent studies (*e.g.*, Gaffen, 1994; Parker and Cox, 1995) pointed out the possible systematic errors and biases of the radiosonde data in monitoring long-term climatic trends and fluctuations, mainly owing to changes of sensors from period to period. However, these studies also have confirmed that the temperature data of the lower troposphere are generally far less influenced by these biases and errors than the stratospheric and the upper tropospheric temperature. Spencer and Christy (1994) examined changes in the global as well as hemispheric mean tropospheric temperature averaged with homogeneously retrieved data from the MSU (Microwave Sounding Units) micro-wave channels on Nimbus satellites. This satellite-derived temperature field has a great advantage in the spatial homogeneity for the whole globe, but the data only cover the period since 1979. This new data set has shown no remarkable trend except large interannual variability related basically to the ENSO cycle. Recently, Parker *et al.* (1997) demonstrated that the vertically-averaged gridded radiosonde temperature in the northern hemisphere, adjusted by MSU-derived temperature, has shown some warming trend in the troposphere, but a remarkable cooling trend in the stratosphere since the 1960s.

These studies suggest that the vertical structure of temperature variation in the troposphere plus the surface needs to be examined, on the basis of the longest-term data set possible. To resolve this problem, in this paper seasonal (3-month) mean air temperatures in the lower troposphere (850, 700, 500 hPa) in the northern hemisphere were analyzed from upper air station data for the period 1964–1993, in combination with gridded surface air temperatures. The aim was to detect and analyze recent temperature trends and inter-decadal-scale variations from the surface to the mid-troposphere. The vertical as well as spatial structure of temperature variations are scrutinized, to elucidate possible forcing factors of these trends and variations.

2. Data and method of analysis

2.1 Data processing

The monthly mean temperatures at the 850, 700, and 500 hPa levels were selected from monthly rawinsonde observation data for north of 20°N in the northern hemisphere for the period from Mar., 1964 to Feb., 1994, using stations with as few missing data as possible. Two-hundreds-twenty-five stations were finally selected (crosses in Fig. 1). These data, up to Dec., 1990, were adopted mainly from the GEDEX CD-ROM (the 1992 version) produced at NASA, and those for Jan., 1991 to Feb., 1994 were taken from Monthly Climatic Data for the World. The distribution of stations used in this study is shown in Fig. 1.

Some of the rawinsonde observation data, particularly in the upper troposphere, have a serious quality-control problem as was pointed out by Gaffen (1994). In addition, the data are sometimes contaminated by non-systematic errors raised during data transmission and/or data editing. To avoid these problems and suppress these errors, all monthly temperatures were checked as follows. The data with anomalies over 4 times of the standard deviation were automatically eliminated, and those over 3 times were compared with the data of neighboring stations and were also eliminated if remarkable differences were found. Through this data processing, the errors in our monthly anomaly data were optimally eliminated and suppressed. The land-based 5° × 5° grid-box monthly surface air temperature compiled by Jones (1994a) was also used.

To calculate monthly mean temperature anomalies of each station and grid-box, the reference period 1977–1986 was used. This averaging period has little missing monthly data. The monthly anomalies at the surface grid box and upper observational stations were averaged to four seasonal (3 month) anomaly values for each season, spring (Mar. to May) summer (Jun. to Aug.) *etc.* The linear trends of seasonal mean temperature in Section 3 were obtained from these seasonal mean anomalies and were calculated by a linear regression based on the 30 years of data. The significance of the trends were examined by t-test assuming that all 30 years of the data were independent.

2.2 Rotated EOF analysis

To deduce the three-dimensional structure and dominant time scales of long-term fluctuation of seasonal temperature change, the Empirical Orthogonal Function (EOF) analysis is applied to the three-dimensional gridded temperature at the four vertical levels. To focus on the decadal-scale fluctua-

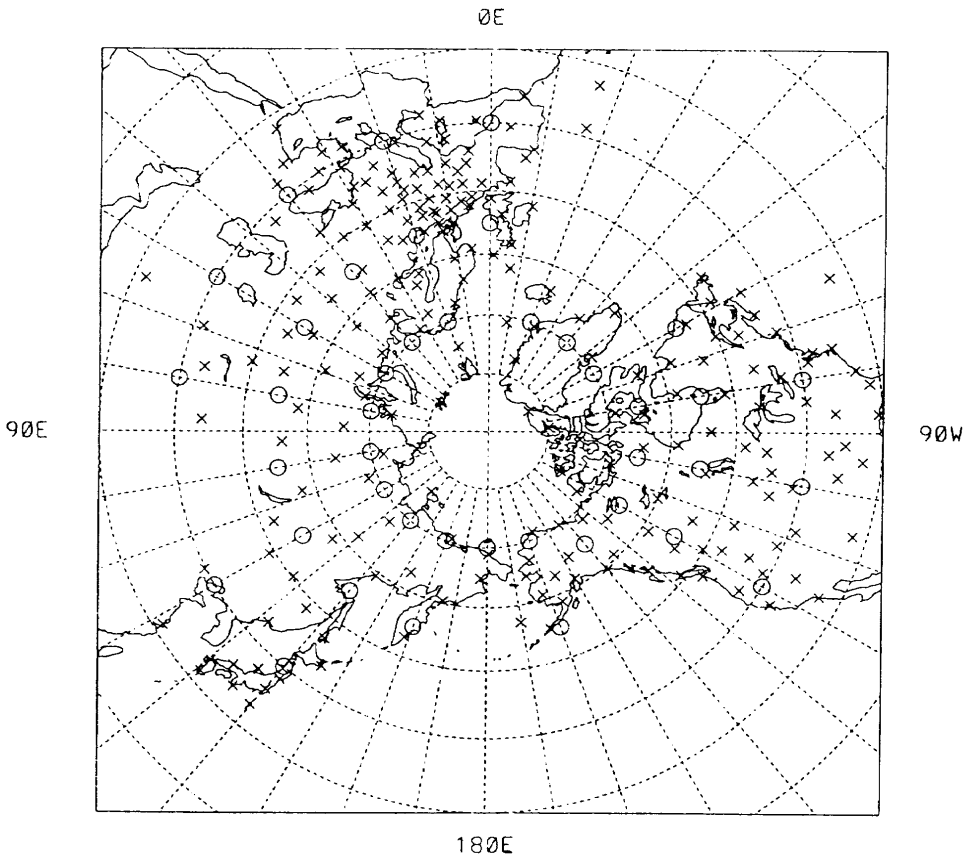

Fig. 1. Distribution of stations (crosses) and interpolated grid points (circles) used in this study.

tion or longer, the seasonal data were low-pass filtered by operating a 5-year moving average. The binomial filter was not used because of some missing data included in each successive 5-years of data. The station and grid-box data were interpolated onto 15° × 20° latitude/longitude grids (open circles in Fig. 1) taken from the filtered data. The grids where original station data are sparse (*i.e.*, ocean areas) are not included in this analysis. In addition, since there are very few stations in Arctic Canada along 70°N between 80°W to 140°W, grids along 65°N were adopted in this region. A total of 41 gridded data were obtained at each level for each year, distributed mainly over the continents. For the EOF analysis, each grid value was weighted by the square root of cosine of latitude, to be proportional to the actual area of individual grid. Variance-covariance matrices were used to calculate eigenvalues and eigenvectors. The contribution of each of the four layers to this analysis are not equal because the anomaly grid data are not divided by their standard deviation. Therefore, the contribution of the surface layer to the obtained EOF mode is slightly larger than those of upper layers because the variance of the surface absolute value is relatively larger.

The EOF analysis of this procedure has a problem of statistical unstable solutions owing to large spatial degree of freedom compared with time domain. In addition, the solutions are made more unstable by using time-filtered data. Barnston and Livezey (1987) described that stable solutions could be obtained generally by applying the rotated EOF analysis to the large spatial grid data. In this study, the relatively stable solutions are obtained by not only rotating but also changing the number of the retained mode. First, the number of rotation is decided according to the method of O'Lenic and Livezey (1988). That is, the relationship between each eigenvalue and its mode number was plotted and five (winter) and six (spring) modes were chosen involving the end of "shelf" (O'Lenic and Livezey, 1988). The five or six EOF mode, explained over 88 % of the total variance in both seasons, were rotated by the varimax method. The rotation was repeated, with the number of the retained mode one or two more and one or two less. As the result, the first two modes in both seasons had the spatial and temporal similarity in every case. This shows the number of rotations were adequate, and neither over rotation nor under rotation occurred. Therefore, these two modes of each season were considered stable. The meaningful climatological interpretations are discussed in Section 4.

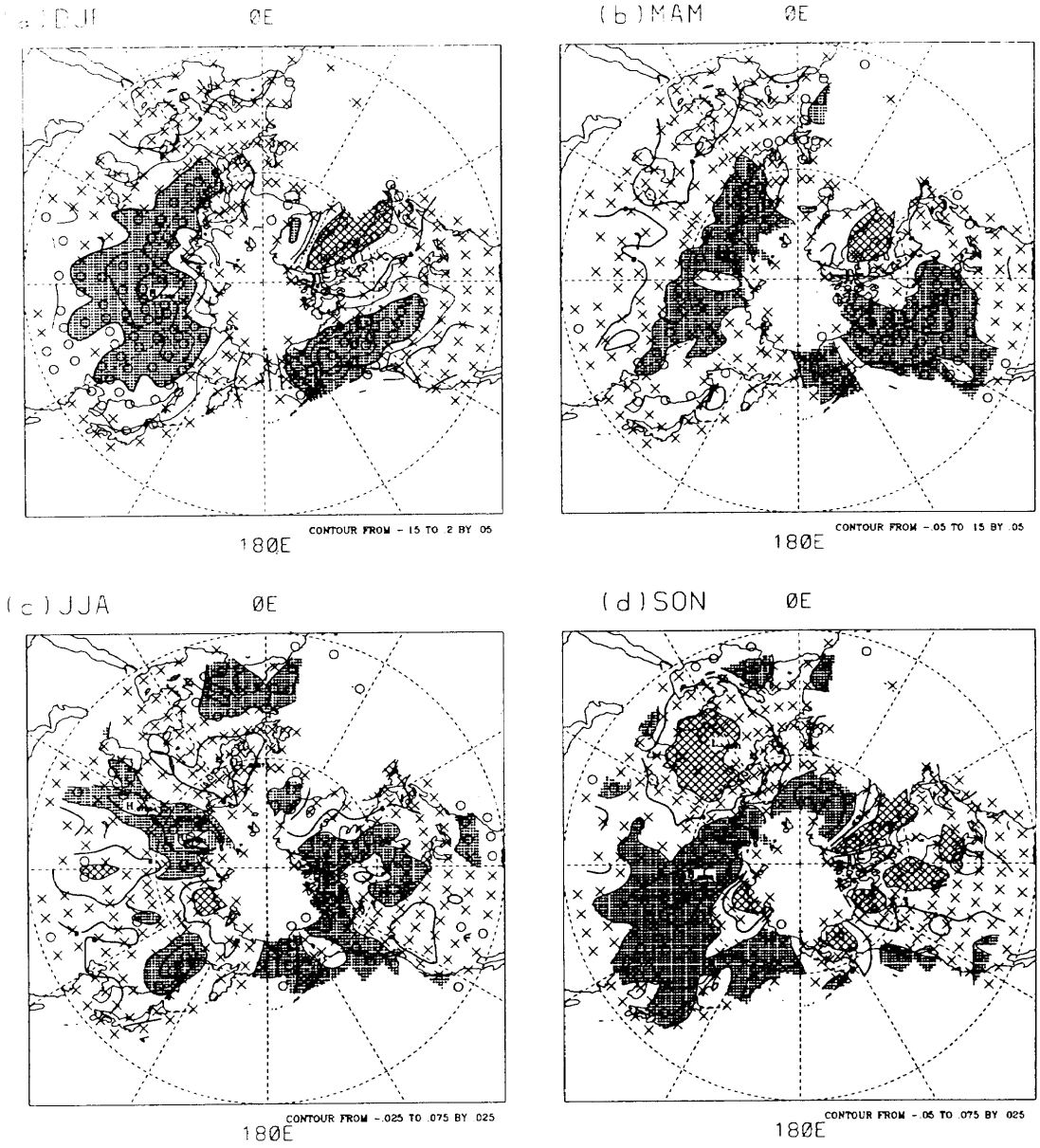

Fig. 2. Spatial distribution of the linear trend of seasonal mean air temperature (1964–1993) at surface. Contour interval is 0.05°C/year for winter and spring and dashed lines indicate negative values. Open circles (crosses) indicate the stations with significance level of 5 % (no significance). Dotted (shaded) areas indicate the value with more (less) than ±0.1°C/year (winter), ±0.05°C/year (spring), or ±0.025°C/year (summer and autumn), respectively. (a) winter, (b) spring, (c) summer, (d) autumn.

3. Linear trends of seasonally-averaged temperature

3.1 Spatial patterns

The spatial as well as vertical structures of linear trends of seasonal-mean temperature during the 30-year period from 1964 to 1993 were examined first at four levels (surface, 850 hPa, 700 hPa and 500 hPa). Figures 2 and 3 show the spatial distribution of linear trend values (°C/year) for spring (March–May), summer (June–July), autumn (September–November) and winter (December–February) at the surface and the 700 hPa level, respectively. For each season, since spatial patterns at the three vertical levels above the surface proved to be more or less similar to each other, only the distributions at 700 hPa level are shown here.

In winter at the surface (Fig. 2a), a significant warming trend is seen over the whole of northern Eurasia and northwest North America. The centers of warming over Eurasia and North America are located over central Siberia and Alaska, respectively, where the maximum values exceed 0.15°C/year. A cooling trend is also noticeable over Arctic Canada through Greenland. These spectacular features in

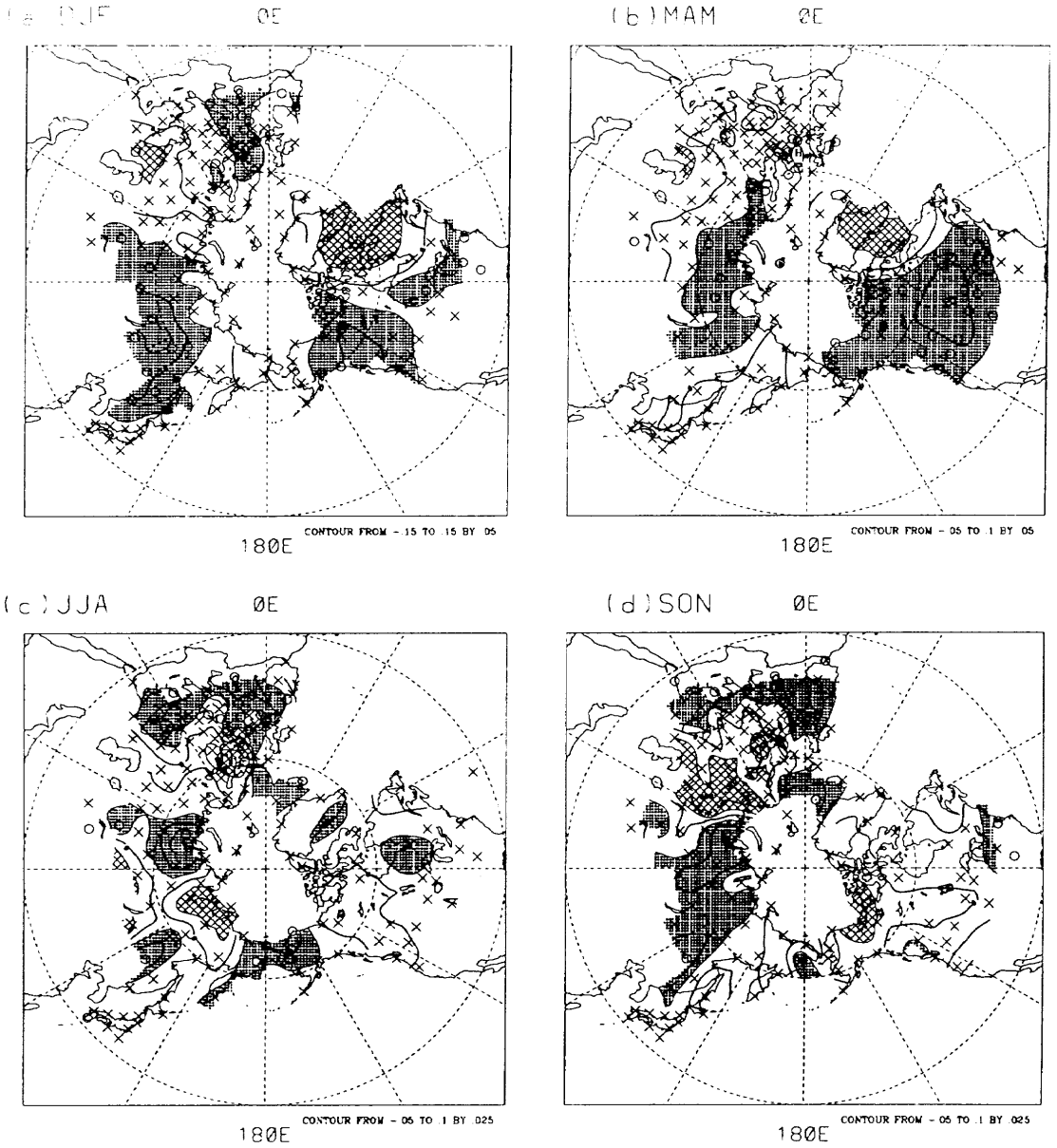

Fig. 3. As in Fig. 2, but for 700 hPa.

winter have already been noted (*e.g.*, IPCC, 1992; 1995). At 700 hPa (Fig. 3a), the overall pattern of warming and cooling areas is consistent with that at the surface, *i.e.*, with the extremes of warming over Siberia and Alaska and an extreme of cooling over the Arctic Canada/Greenland area. Another area of warming and cooling was also noted over western Europe and central Asia between the Black Sea and the Caspian Sea, respectively. That is, a more wavy structure of positive and negative trends is recognized at this level than the surface over the Eurasian continent.

In spring, an overall warming trend is noticeable at the surface level (Fig. 2b), with notable warming areas over North America and the northern Eurasia, *i.e.*, the East European Plain through central Siberia. The warming trend is more remarkable over North America than over Eurasia, which is in contrast with the feature in winter. At 700 hPa (Fig. 3b), these warming areas at the surface level are also apparent with the extreme value over central Canada. Areas of cooling trends are also noticeable over Greenland and central Asia, which are similar to those in winter.

In summer (Figs. 2c and 3c), the overall feature is more complex and less significant than the other seasons, both at the surface and 700 hPa. The areas with significant warming trend are commonly apparent at the two levels in southern Europe, at the Ob River basin, and around the Bering Sea, though degrees of warming are not so large (with less than 0.05°C/year in most areas). Over the Arctic Canada

region the warming trend is apparent at the surface, but no significant trend is seen at 700 hPa. Areas with cooling trends are not seen except for small areas over Mongolia and northeastern Siberia.

In autumn at the surface (Fig. 2d), a warming trend is seen over a wide area of central Siberia and southern Europe. In contrast to during winter and spring, no warming trend is seen over North America. Areas with a cooling trend are seen over the western half of Eurasia (30°E to 60°E) and northwestern North America. The overall feature at 700 hPa (Fig. 3d) is very similar to that at the surface, though the positive/negative patterns are not so significant and dominant as those at the surface.

It should be noted that over Eurasia the patterns of this season are very similar to those in winter, whereas over North America the similarity of the spatial patterns is not seen between winter and autumn but more remarkably seen between winter and spring.

3.2 Vertical structure of trends in winter and spring

As shown in the previous subsection, the overall pattern (particularly of warming trend) has proved to be significant at middle and high latitudes in winter and spring. In this sub-section the vertical structure of a linear trends is scrutinized. Figure 4 shows the vertical-longitude section of a linear trend in winter for every 10 degree latitude band from 70°N to 40°N.

At 70°N (Fig. 4a), remarkable warming trends predominate over North America centered at 120°W, especially at the lowermost part of the troposphere (*i.e.*, 850 hPa). At 60°N (Fig. 4b) warming trends are most remarkable both over Eurasia centered at 120°E (central Siberia) and over North America centered at 120°W, particularly in the lower troposphere (surface to 850 hPa). Over Siberia, a large increasing trend (of more than 0.15 °C/year) reached the 700 hPa level. A cooling trend located over eastern Canada to Greenland near 60°W through the lower troposphere. At 50°N (Fig. 4c), a warming trend of more than 0.1 °C/year was seen over a broad region of Siberia, but over North America the warming trend was confined at and near the surface level of the west coast area.

Figure 5 shows the same diagram as Fig. 4 but for spring. In this season, the warming trend predominates only over the North American sector, (90°–120°W) with the largest values in the lower troposphere (surface to 700 hPa) of 50°N–70°N latitudes. Over the Eurasian sector, warming trends are very limited near the surface level of the 70°N latitude belt. Cooling trends over Greenland centered at 60°W are dominant throughout the lower troposphere. A relatively small cooling trend is noticed at 500–850 hPa levels over east Siberia (70°N–60°N), though this trend is not apparent at the surface.

These results have shown that warming trends during the recent 30 years have been noticeable not only at the surface but also through much of the lower troposphere of the northern hemisphere. The hemispheric patterns of warming (and cooling) trends agree fairly well with those of the surface air temperature, particularly in winter and spring, though some differences in the vertical structure are also noticed from region to region, as well as from season to season.

4. Three-dimensional patterns of long-term fluctuations in winter and spring

The temperature field in winter and spring has shown remarkable warming trends through the lower troposphere. To deduce the vertical as well as horizontal structure and dominant time scales of the long-term fluctuation in these seasons, three-dimensional rotated EOF analysis was applied to the gridded temperature anomalies at four levels. The data procedure is described in Section 2.

4.1 Winter

Figure 6 shows the spatial patterns (factor loading) for each level for the first component, which occupies about 30 % of the total variance. At the surface level (Fig. 6a), a broad area of large positive values is located over the large part of Eurasia. Another area of positive values is seen over Alaska and northwest Canada, though its spatial-scale is smaller than that over Eurasia. This positive/negative pattern is fundamentally the same for 850, 700 and 500 hPa levels, though the spatial variances gradually diminish upward, particularly over Eurasia. Small areas of negative values are seen only at 500 and 700 hPa levels over Scandinavia and northeastern Siberia.

The time coefficients (scores) of this component are shown in Fig. 7. The figure shows an increasing trend through the recent 30 years, especially in the 1970s. That gives a monotonic warming trend at the surface over the whole of Eurasia and at the lower troposphere over Siberia, centered over the Lena/Yenisei River basins. Another center of steady warming is located over Alaska/northwest Canada, with less spatial extent and amplitude. It should be noted that after around 1990, this warming trend has been weakened.

Figure 8 shows the spatial pattern (factor loading) of each level for the second component, which occupies about 25 % of the total variance. This mode chiefly depicts temperature change from the northern part of North America to the the European sector, showing a dipole or wavy structure with a deep negative center over northeast Arctic Canada and a large positive center over Scandinavia. Another broad area with positive values is seen over southern Siberia and East Asia. Eastern North America

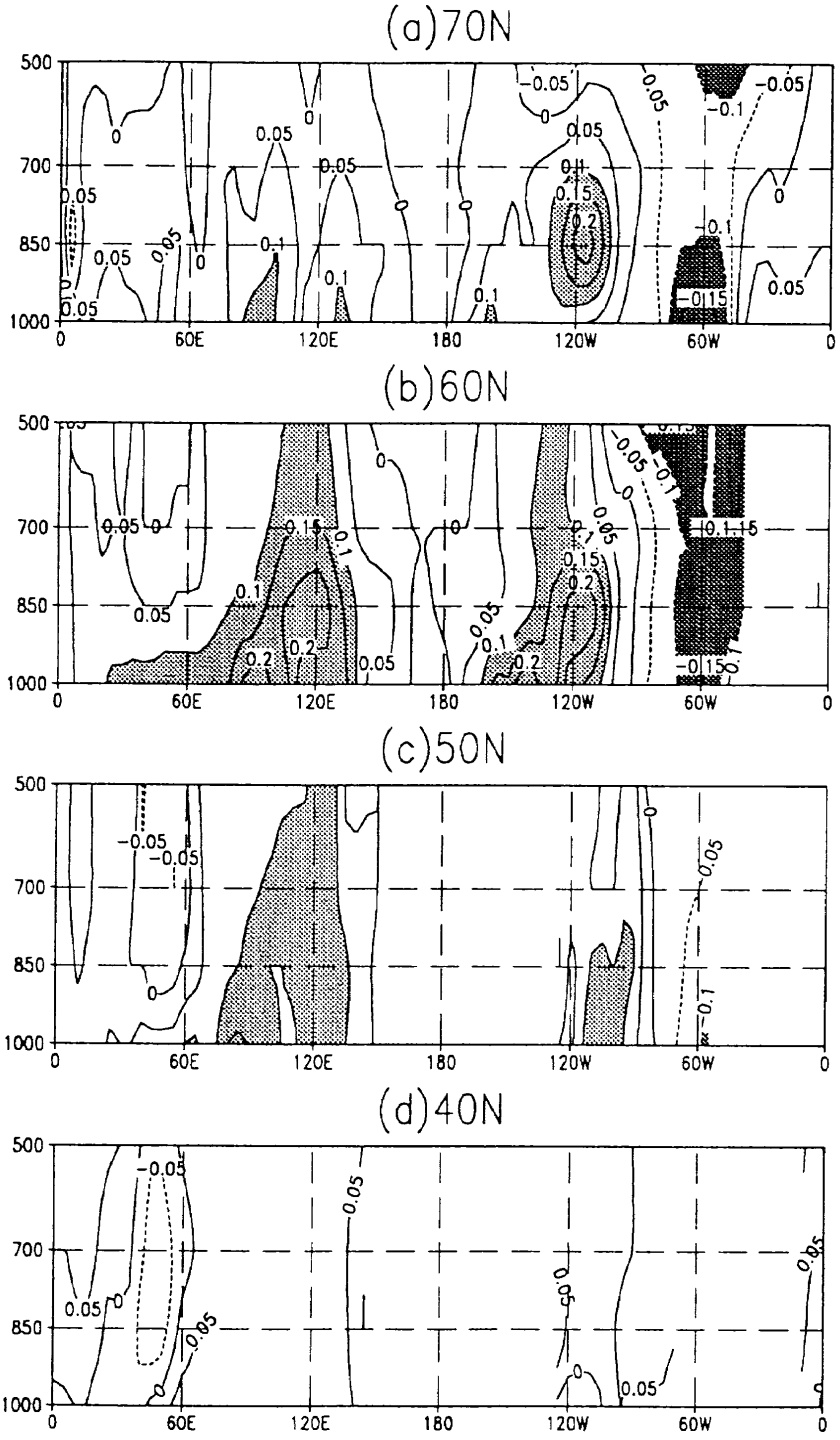

Fig. 4. Longitude-altitude section of linear trends of seasonal mean air temperatures (1964–1993) in each latitude belt in winter. Contour interval is 0.05°C/year and dashed lines indicate negative values. Dotted (shaded) areas indicate the values with more (less) than 0.1 (−0.1)°C/year.

also shows a positive center, though the real center is likely to be to south of 40°N. Roughly speaking, the overall spatial pattern looks like a stationary wavenumber three pattern, though the amplitude over the European sector is extremely large.

The vertical structures from the surface to 500 hPa are similar to each other, with small amplitude changes toward the upper level. These features in the horizontal as well as vertical structures of this mode strongly suggest that this mode in the temperature change is closely associated with a barotropic-type stationary wave response of the atmosphere induced by some dynamic forcing outside of this region. This aspect will be discussed further in the next section.

The time coefficients of this component are also

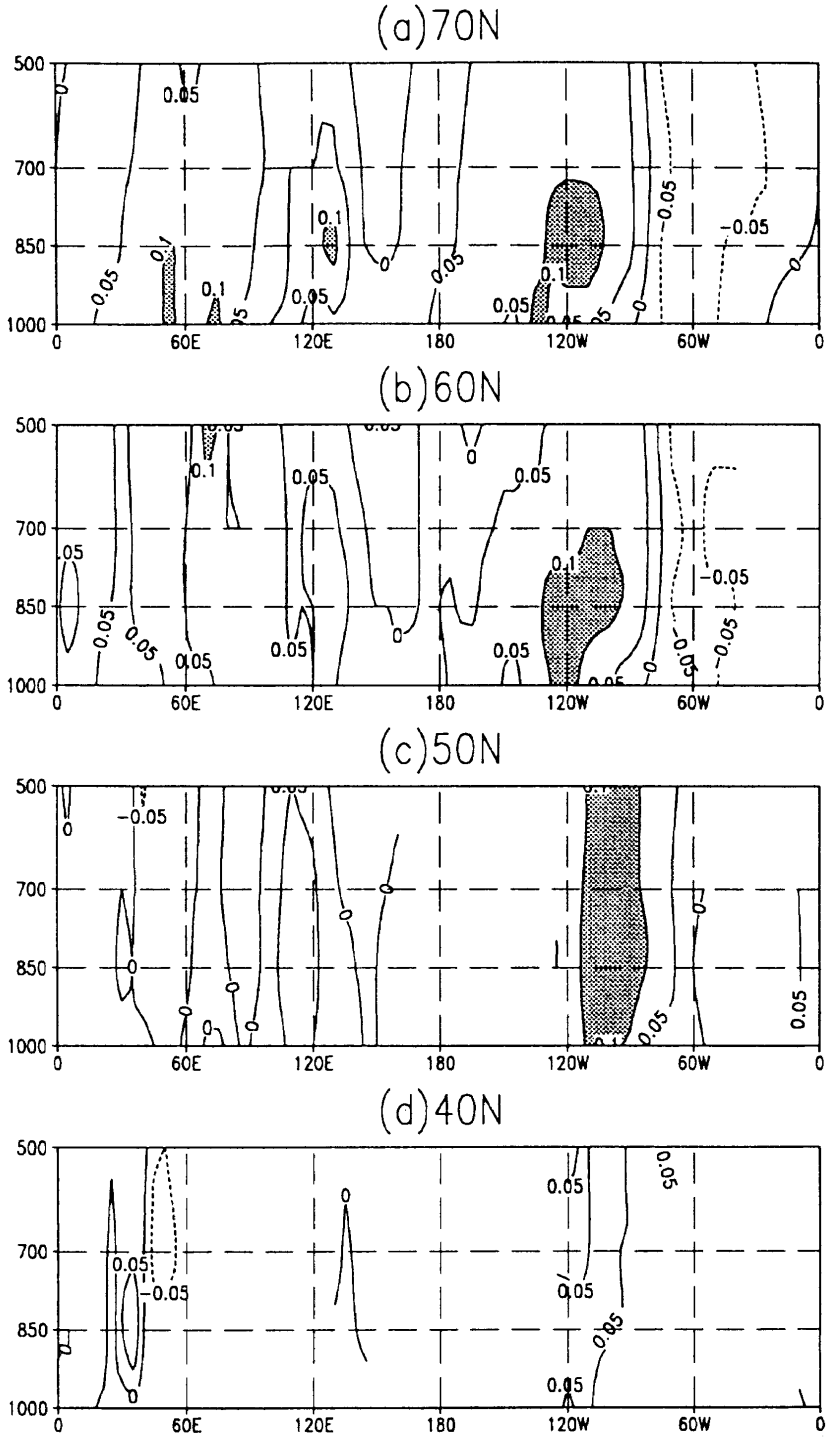

Fig. 5. As in Fig. 4, but for spring.

shown in Fig. 7, which clearly demonstrates an interdecadal scale fluctuation with a maximum in the early 1970s, a rapid decrease in the middle 1970s and a rapid increase in the late 1980s. That is to say, the temperature over the northeast north America (Scandinavia) was relatively high (low) in the late 1970s through the early 1980s, but it changed to the reversed pattern after the late 1980s. It should be noted here that in East Asia, winter temperature anomalies decreased after the 1976/77 winter and became positive after 1988/89 (Japan Meteorological Agency, 1994). This temperature change in east Asia including Japan seems to be well represented by this mode, where weak positive values are shown in Fig. 7. Recently, a similar feature was described by Kachi and Nitta (1997).

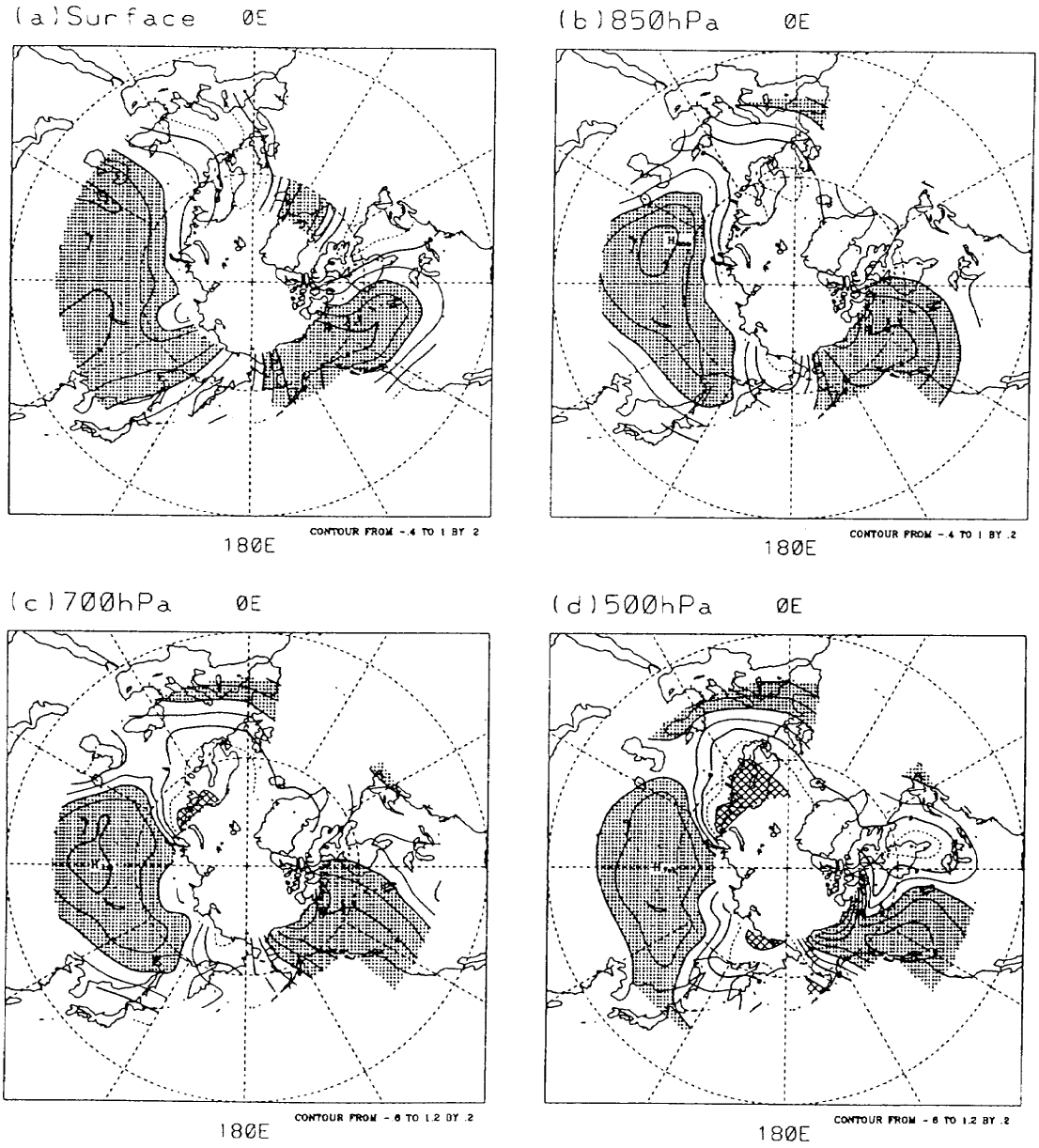

Fig. 6. First three-dimensional factor loadings derived by the rotated EOF for 5-year running mean temperature anomalies in winter. Contour interval is 0.2 and dashed lines indicate negative values. Dotted (shaded) areas indicate the values with more (less) than 0.4 (−0.4). (a) surface, (b) 850 hPa, (c) 700 hPa, (d) 500 hPa.

4.2 Spring

Figure 9 shows the spatial pattern (eigen vectors) of each vertical level for the first component, which occupies about 26 % of the total variance. A remarkable positive anomaly is located over northern North America and a relatively smaller negative anomaly over the northwestern part of Europe. The overall spatial patterns at the surface to 500 hPa are similar to each other, but a large area of negative anomaly is seen over Eastern Siberia in the middle troposphere (500 hPa). The time variation of this component (Fig. 10) shows an increasing trend with some decadal-scale fluctuation, implying a warming trend over the positive anomaly areas, *i.e.*, northern North America.

The spatial pattern of the second component, which occupies about 20 % of the total variance, is shown in Fig. 11. Time coefficients are also shown in Fig. 10. This pattern represents relatively localized temperature change. Three positive values are seen over the Aleutian low area, central Siberia near Lake Baikal, and southwestern parts of Europe. A negative area is seen from Greenland to Scandinavia, remarkably in the middle troposphere. It is interesting to note that the time variation of this component shows a 10–13 year period oscillation (Fig.

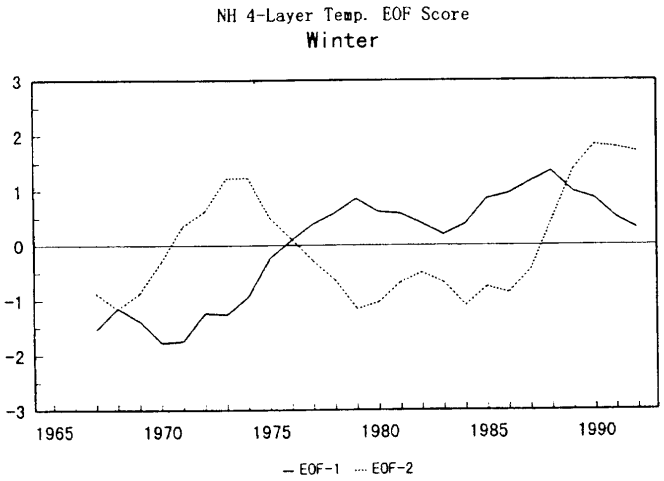

Fig. 7. Time coefficients (*i.e.*, component scores) of the first two components in winter.

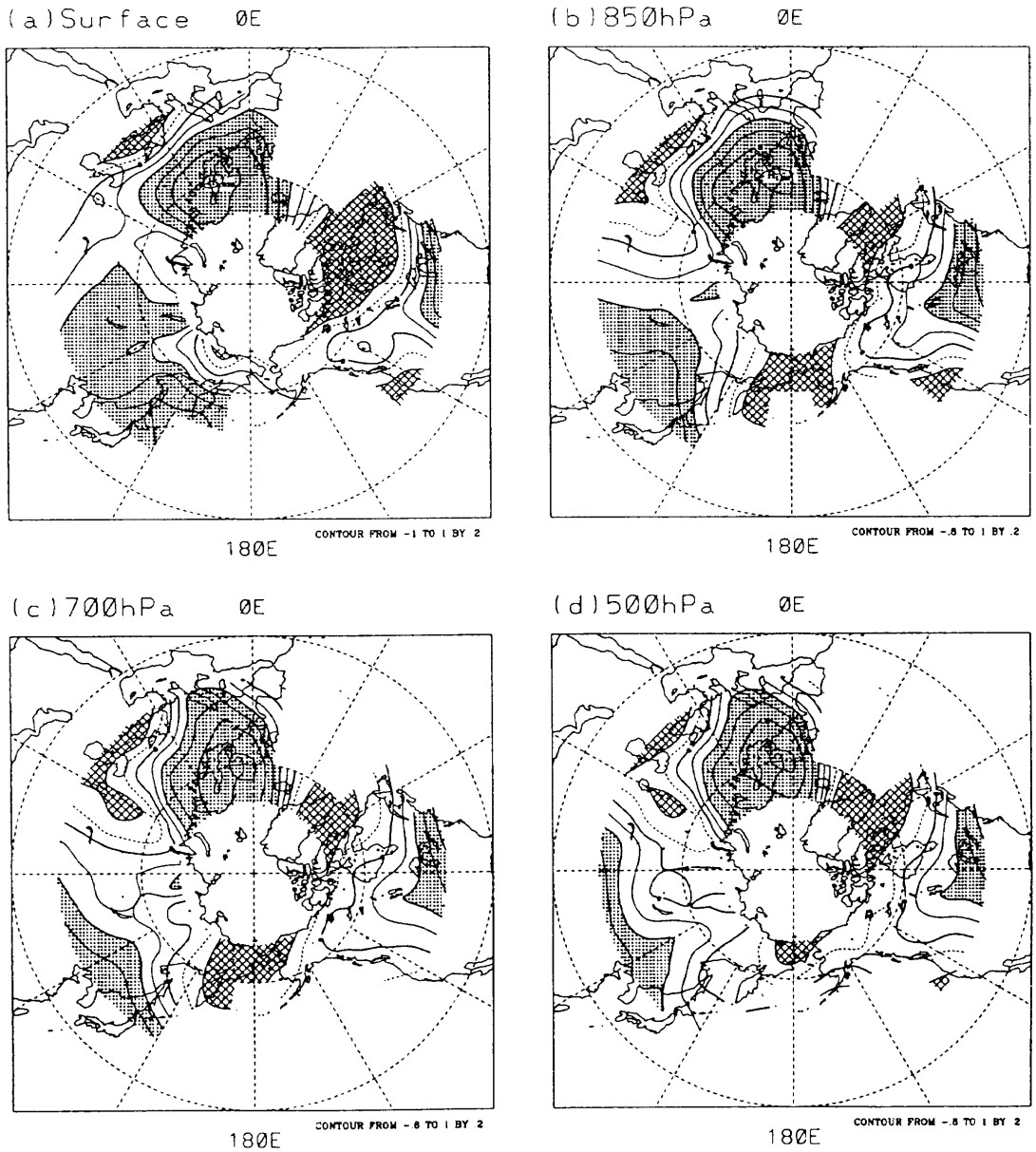

Fig. 8. As in Fig. 6, but for second component.

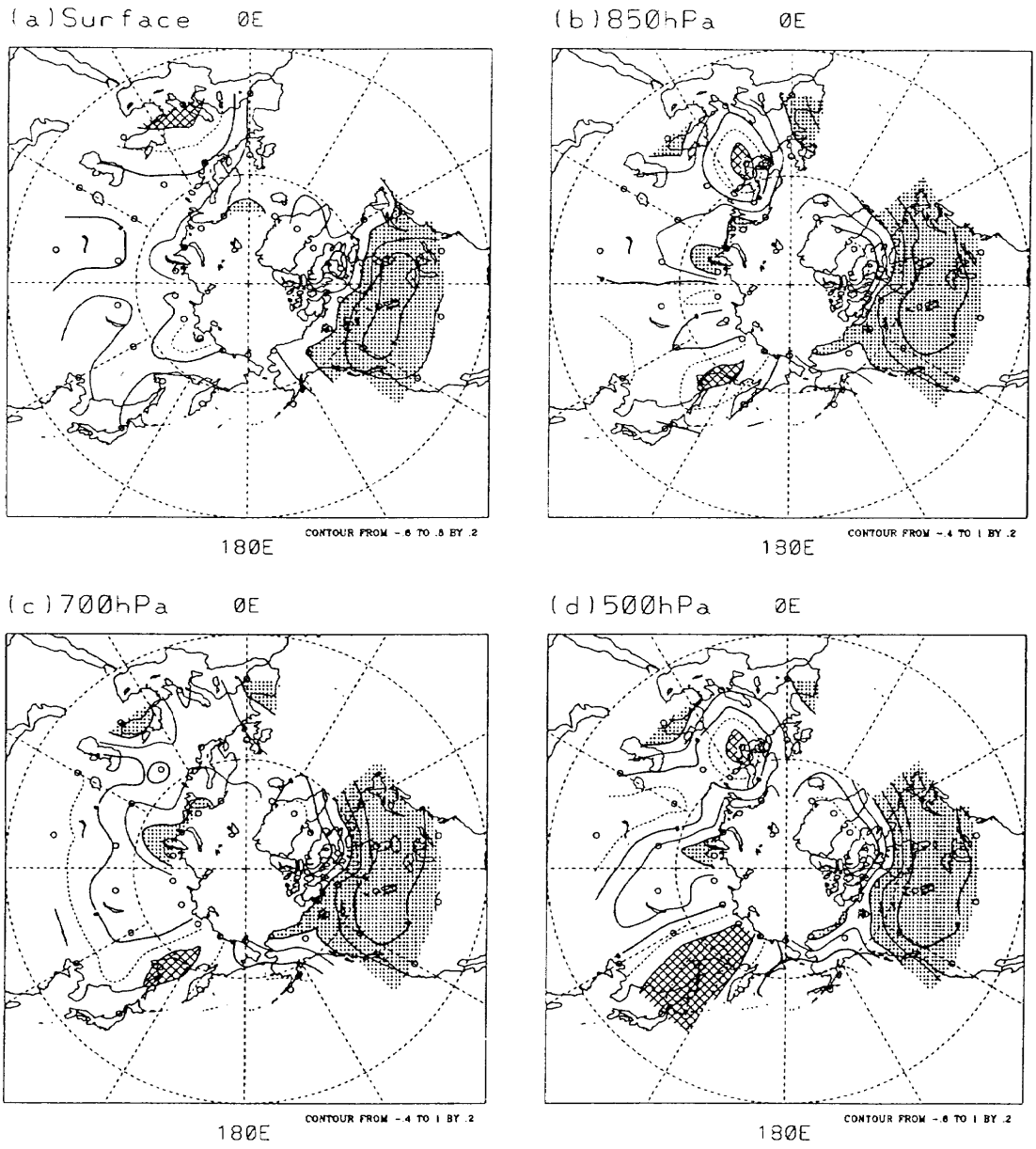

Fig. 9. As in Fig. 6, but for first component in spring.

10), which appears to correspond with the solar cycle variation with sun-spot maxima in late 1960s, around 1980, and in the late 1980s. This feature will further be discussed in a separate paper.

5. Summary and discussion

By using the radiosonde station data for the recent 30 years (1964–93) in the northern hemisphere, the horizontal and vertical structures of the combined surface and the lower tropospheric temperature field were analyzed to detect and specify trends and decadal-scale fluctuations. The linear trend analysis has shown that the overall warming is apparent over the continents in northern winter and spring, with significant maxima over Siberia and Arctic Canada/Alaska region. The warming tendency is most remarkable at the surface and in the lowermost troposphere (850 hPa) over Siberia, whereas it is more equally apparent through the lower-half of the troposphere over North America.

The three-dimensional rotated EOF analysis in winter has revealed the two independent modes. The first mode (30 % of the total variances) represents a warming trend over Siberia and northwest Canada, combined with a cooling trend near Greenland. The second mode (25 % of the total variances) represents a decadal-scale fluctuation of the tropospheric temperature, associated with the atmospheric circulation change over the north Pacific and the North Atlantic regions.

In spring, a dominant mode of warming trend in the rotated EOFs has appeared only over the whole

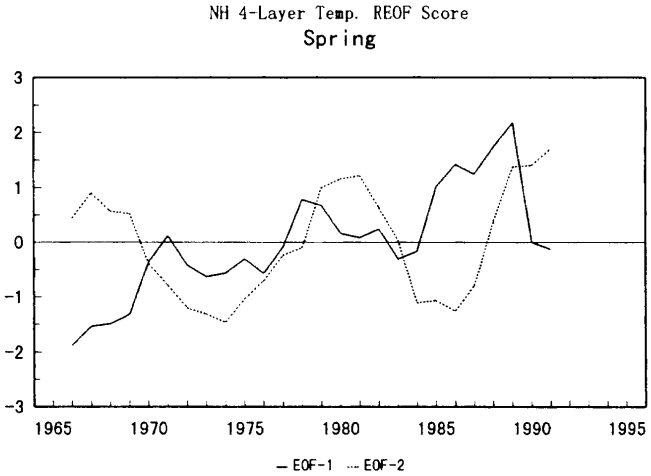

Fig. 10. As in Fig. 7, but for first two components in spring.

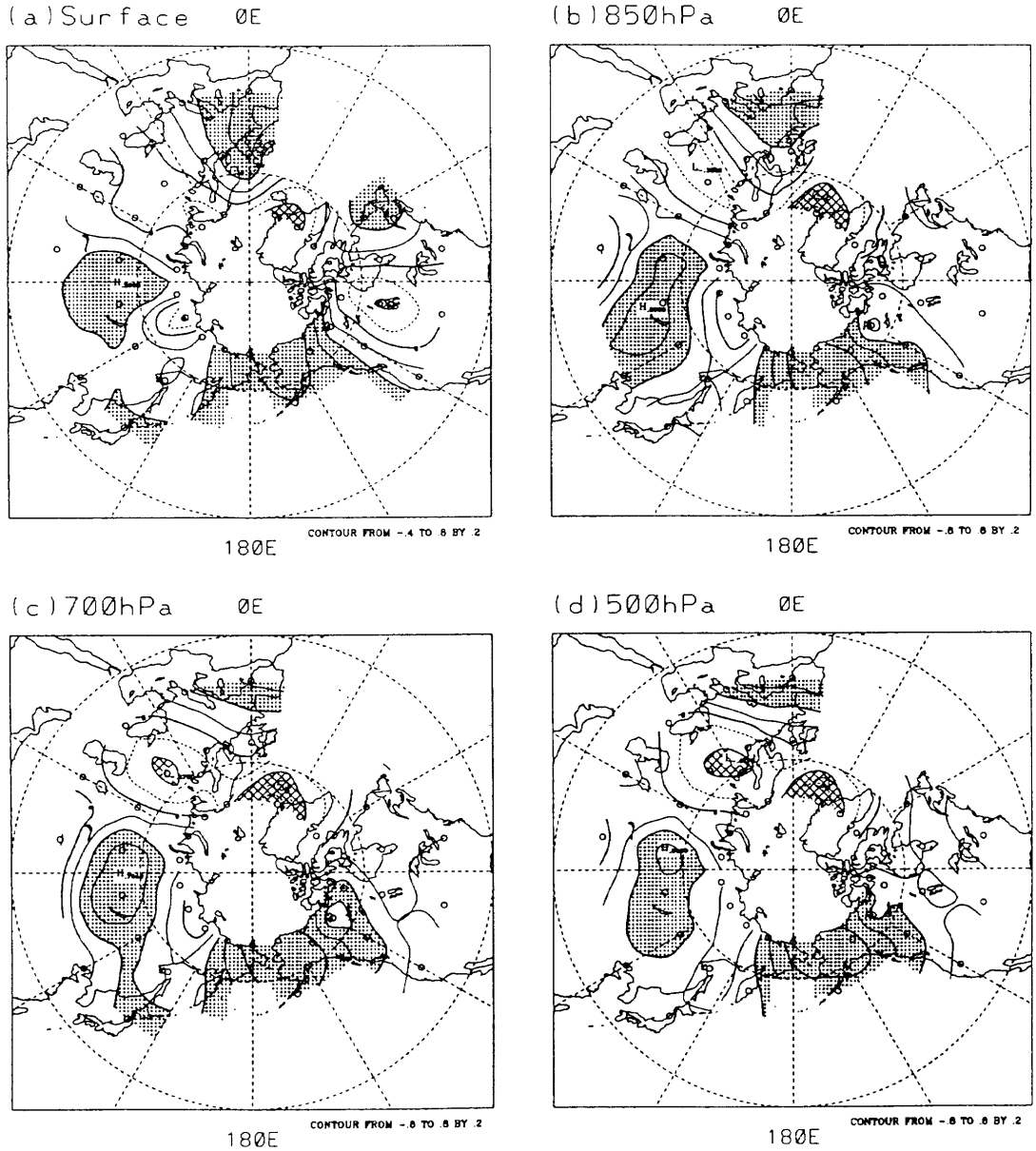

Fig. 11. As in Fig. 6, but for second component in spring.

of Canada, which occupies 26 % of the total variances. Over the Eurasian continent and Alaska, inter-decadal scale fluctuations with 10–13 year period are more prominent, a fact represented in the second component of the EOFs.

The dominant modes in the tropospheric temperature field in northern winter and spring might be related to the different feedback processes in the climate system. The first mode in winter and spring show a more or less monotonically increasing trend. An issue may be whether this increasing temperature trend is directly related to the gradually-intensified greenhouse effect due to the increase of CO_2, CH_4 and other greenhouse gases. This important issue should be examined more quantitatively, including by model computation.

It should be noted, however, the areas of remarkable warming (*i.e.*, Siberia and Alaska) in winter correspond well with the areas of strong near-surface inversion layer formed by strong surface radiative cooling. In addition, this mode shows larger amplitudes at the surface and near-surface level (*i.e.*, 850 hPa) compared to the upper levels (700 and 500 hPa levels). In spring, in contrast, the nearly-linear warming trend is apparently seen only over Canada, with more uniform vertical strucure of anomalies from the surface to 500 hPa level. These differences of the warming trends in the three-dimensional structure and seasonality should be considered in assessing the forcing factors of temperature fluctuations.

Rogers and Thompson (1995) noted the increased Atlantic Arctic cyclone activity during 1980s is closely related to the warming over Siberia in winter, possibly through warm air advection in the cyclone warm sectors. The stronger westerly flow aloft may also be responsible for breaking down the cold surface inversion. However, this change of atmospheric circulation does not necessarily imply that warming by the greenhouse effect over Siberia is negligible or less important. Or rather, this circulation change may have been a result of radiative anomalous warming over there. In fact, near-surface radiative warming due to increase of greenhouse gases may possibly be actualized selectively in space and season (*e.g.*, IPCC, 1995), although the changes of the gas concentrations might be occurring more or less uniformly over the whole globe due to relatively-rapid diffusion processes in the atmosphere. The strong and broad near-surface inversion layer in winter in the interior of the continent, such as Siberia and northwest Canada and Alaska, is likely to provide the most suitable condition for the greenhouse effect. The contrastive cooling trend over northeast Canada and Greenland, which also appeared in this mode, may be associated with re-adjustment of the Arctic cold polar vortex to the warming over Siberia and northwest Canada. We need, however, to examine atmospheric circulation changes and other natural forcing factors such as sea surface temperature forcing in the tropics and the extra-tropics, to fully understand the increasing trend and decadal-scale fluctuations of the tropospheric temperature field.

The inter-decadal fluctuation in winter as shown in the second component is another prominent feature in the tropospheric temperature field in the recent 30 years. This mode is likely to be closely related to the hemispheric atmospheric circulation field of the same time-scale, combined with the two drastic changes (or "climatic jumps") between 1976/77 and 1988/89, which have been discussed in some recent studies (Kodera *et al.*, 1996; Kachi and Nitta, 1997; Tanaka *et al.*, 1997; Watanabe and Nitta, 1997 *etc.*). In fact, positive temperature anomalies in the Alaska/Bering Sea region in the period between 1976/77 and 1988/89, as suggested in the combination of spatial pattern and time coefficient, correspond well with the warm advection effect caused by the persistently stronger-than-normal Aleutian low in this period (Wallace *et al.*, 1993; Trenberth and Hurrel, 1994; Tachibana *et al.*, 1996). This inter-decadal fluctuation is likely to be confined in winter, since this mode did not appear in the dominant modes of the other seasons. The temperature anomaly over the North Atlantic seems be closely related to the decadal change of the NAO (Hurrel, 1994).

The 10–13 year oscillation is another notable feature in the temperature field in spring, with the maximum temperature anomaly in central Siberia and the Alaska/Bering Sea region in late 1960s, around 1980 and around 1990. The time sequence of this mode happened to correspond with the solar cycle variation with sun-spot maxima in late 1960s, around 1980 and late 1980s, though the record of 30 years may be too short to relate to the solar cycle, which has a period of about 11 years. These aspects need be examined further, by using many other data sets, such as stratosphere data sets.

References

Angell, J.K., 1988: Variations and trends in tropospheric and stratospheric global temperatures, 1958–87. *J. Climate*, **1**, 1296–1313.

Barnston, A.G. and R.E. Livezey, 1987: Classification, seasonality and persistence of low-frequency atmospheric circulation patterns. *Mon. Wea. Rev.*, **115**, 1083–1126.

Gaffen, D.J., 1994: Temporal inhomogeneities in radiosonde temperature records. *J. Geophys. Res.*, **99**, 3667–3676.

Hansen, J. and S. Lebedef, 1987: Global trends of measured surface air temperature. *J. Geophys. Res.*, **92D**, 13345–13372.

Hurrell, J.W., 1995: Decadal trends in the North Atlantic Oscillation: Regional temperatures and precipitation. *Science*, **269**, 676–679.

IPCC, 1996: Climate Change 1995: *The Science of Climate Change*. J.T. Houghton *et al.* (Eds.), Cambridge University Press, Cambridge, UK, 572 pp.

Japan Meteorological Agency, 1994: *Report on Recent changes in the World 1994—Reviews and Outlook for the Future—(V)*. Printing bureau of the Ministry of Finance, 444 pp (in Japanese).

Jones, P.D. and K.R. Briffa, 1992: Global surface air temperature variations during the twentieth century: Part 1, spatial, temporal and seasonal details. *Holocene*, **2**, 165–179.

Jones, P.D., 1994a: Hemispheric surface air temperature variations: A reanalysis and an update to 1993. *J. Climate*, **7**, 1794–1802.

Jones, P.D., 1994b: Recent warming in global temperature series. *Geophys. Res. Lett.*, **21**, 1149–1152.

Kachi, M. and T. Nitta, 1997: Decadal variations of the global atmosphere-ocean system. *J. Meteor. Soc. Japan*, **75**, 657–675.

Kodera, K., M. Chiba, H. Koide, A. Kitoh and Y. Nikaidou, 1996: Interannual variability of the winter stratosphere and troposphere in the Northern Hemisphere. *J. Meteor. Soc. Japan*, **74**, 365–382.

Nitta, T. and S. Yamada, 1989: Recent warming of tropical sea surface temperature and its relationship to the Northern Hemisphere circulation. *J. Meteor. Soc. Japan*, **67**, 375–383.

O'Lenic, E.A. and R.E. Livezey, 1988: Practical considerations in the use of rotated principal component analysis (RPCA) in diagnostic studies of upper-air height fields. *Mon. Wea. Rev.*, **116**, 1682–1689.

Oort, A.H. and H. Liu, 1993: Upper-air temperature trends over the globe, 1958–89. *J. Climate*, **6**, 292–307.

Parker, D.E., P.D. Jones, C.K. Folland and A. Bevan, 1994: Interdecadal change of surface temperature since the late nineteenth century. *J. Geophys. Res.*, **99D**, 14373–14399.

Parker, D.E. and D.I. Cox, 1995: Towards a consistent global climatological rawinsonde data-base. *Int. J. Climatol.*, **15**, 473–496.

Parker, D.E., M. Gordon, D.P.N. Cullum, D.M.H. Sexton, C.K. Folland and N. Rayner, 1997: A new global gridded radiosonde temperature data base and recent temperature trends. *Geophys. Res. Lett.*, **24**, 1499–1502.

Rogers J.C. and E. Mosley-Thompson, 1995: Atlantic Arctic cyclones and the mild Siberian winters of the 1980s. *Geophys. Res. Let.*, **22**, 799–802.

Spencer, R.W. and J.R. Cristy, 1992: Precision and radiosonde validation of satellite gridpoint temperature anomalies, Part II: A tropospheric retrieval and trends during 1979–90. *J. Climate*, **5**, 858–866.

Tanaka, H., R. Kanohgi and T. Yasunari, 1996: Recent abrupt intensification of the northern polar vortex since 1988. *J. Meteor. Soc. Japan*, **74**, 947–954.

Tachibana, Y., M. Honda and K. Takeuchi, 1996: The abrupt decrease of the sea ice over the southern part of the Sea of Okhotsk in 1989 and its relation to the recent weakening of the Aleutian Low. *J. Meteor. Soc. Japan*, **74**, 579–584.

Trenberth, K.E. and J.W. Hurrel, 1994: Decadal atmosphere-ocean variations in the Pacific. *Climate Dyn.*, **9**, 303–319.

Wallace, J.M., Y. Zhang and K.-H. Lau, 1993: Structure and seasonality of interannual and interdecadal variability of geopotential height and temperature fields in the Northern Hemisphere troposphere. *J. Climate*, **6**, 2063–2082.

Walsh, J.E., W.L. Champman and T.L. Shy, 1996: Recent decrease of sea level pressure in the central Arctic. *J. Climate*, **9**, 480–486.

Watanabe, M. and T. Nitta, 1997: Recent climate changes and associated decadal variations in the Northern Hemisphere winter. *Tenki*, **44**, 208–212. (in Japanese)

過去 30 年間 (1964–1993) における北半球の地表面および下部対流圏気温の長期傾向と 10 年スケールの変動

安成哲三・西森基貴
（筑波大学地球科学系）
水戸哲司[1]
（筑波大学環境科学研究科）

過去 30 年間 (1964–93) の北半球における地表面と下部対流圏の気温変動を解析した結果、冬季と春季を中心に地表面のみならず、下部対流圏全体で顕著な昇温傾向が確認された。冬季には、中央シベリアとカナダ西北部・アラスカで昇温が顕著であるが、両地域における昇温の鉛直構造に大きな違いが見られた。春季には北米大陸北半部でのみ、下部対流圏全体にわたる昇温が顕著である。

地表面から対流圏中部までの気温変動についての 3 次元回転 EOF 解析をした結果、地表面・対流圏全体で昇温するトレンドが最も卓越している変動であることが確認された。回転 EOF 解析の第 2 成分とし

て、冬季には1976/77と1988/89頃に偏差が大きく変化する数10年スケールの長期変動が存在し、その空間特性は北米、北ヨーロッパおよびユーラシア東部で同じ変動傾向を示す波数3型の構造をしていることが示された。一方春季の第2成分は、10–13年周期の変動を示し、太陽活動の同じ周期帯の変動との関連が示唆された。

[1]現在所属：東京電力